

# Technical Notes

TECHNICAL NOTES are short manuscripts describing new developments or important results of a preliminary nature. These Notes cannot exceed 6 manuscript pages and 3 figures; a page of text may be substituted for a figure and vice versa. After informal review by the editors, they may be published within a few months of the date of receipt. Style requirements are the same as for regular contributions (see inside back cover).

## Coupling Conditions for Integrating Boundary Layer and Rotational Inviscid Flow

Peter M. Sockol\*

NASA Lewis Research Center, Cleveland, Ohio  
and

William A. Johnston†

Aerospace Corporation, El Segundo, California

### Introduction

IN recent years, interacting boundary-layer methods have been used to obtain good agreement between prediction and experiment for a variety of flows in which a thin shear layer interacts with an irrotational freestream. Many of the significant achievements in this area have been reviewed by Melnik.<sup>1</sup> There are, however, important classes of flows where the effects of freestream rotationality are significant. These include flows with shocks strong enough to separate the boundary layer and flows in turbomachinery where a nonuniform core is produced as the cumulative result of the action of upstream blade rows. With the development of new, more efficient Euler equation solvers, there is now increased interest in extending interacting boundary-layer techniques to these more general flows.

In a previous Note,<sup>2</sup> we suggested a procedure for obtaining coupled boundary-layer and Euler equation solutions. The procedure utilized transpiration boundary conditions for the inviscid flow in which surface-normal fluxes of mass, streamwise momentum, and total enthalpy were specified. The values of these fluxes were obtained from matching viscous and inviscid solutions. For a growing displacement thickness, these three relations provide the correct number of external conditions at a subsonic inflow boundary. For a decreasing displacement thickness, such as occurs downstream of an airfoil trailing edge, the three relations represent an overspecification because the Euler equations permit only one external condition at a subsonic outflow boundary. Recently, Murman and Bussing<sup>3</sup> have examined various forms for the coupling conditions between the boundary-layer and Euler equation solutions. Although many of the issues concerning these different treatments are well discussed, the question of what to use remains open.

In the present work, we re-examine the matching of a boundary layer and a rotational inviscid flow. Our earlier coupling conditions are extended to include the case where the boundary-layer solution includes the second-order effects of the freestream vorticity and total temperature gradient. It is then shown that two of the three conditions are not independent. If the boundary-layer solution satisfies the appropriate momentum and energy integral relations, then the

imposition of the normal mass flux condition insures that the conditions on a normal flux of streamwise momentum and total enthalpy will also be satisfied. Finally, we describe a consistent procedure for determining the two remaining external boundary conditions required at a subsonic inflow surface.

### Analysis

We consider the flow in the neighborhood of an impermeable wall and write the boundary-layer equations in locally Cartesian coordinates with  $x$  parallel and  $y$  normal to the wall,

$$(\rho u)_x + (\rho v)_y = 0 \quad (1)$$

$$(\rho u^2)_x + (\rho uv)_y + p_x = \tau_y \quad (2)$$

$$p_y \approx 0 \quad (3)$$

$$(\rho u H)_x + (\rho v H)_y = q_y + (u\tau)_y \quad (4)$$

where  $u$  and  $v$  are the  $x$  and  $y$  velocity components, respectively, the  $\rho$  density,  $p$  the pressure,  $H$  the total enthalpy,  $\tau$  the shear stress, and  $q$  the heat flux. At the wall,  $y=0$  and

$$u_0 = v_0 = 0 \quad (5a)$$

$$H_0 \text{ or } (H_y)_0 \text{ specified} \quad (5b)$$

At the edge of the boundary layer,  $y=\delta$ ,

$$u_y \rightarrow u_y^m = -\omega_0^i \quad (6a)$$

$$H_y \rightarrow H_y^m = (H_y)_0^i \quad (6b)$$

where  $m$  denotes an outer matching value and  $\omega_0^i$  and  $(H_y)_0^i$  the wall values of the inviscid vorticity and total enthalpy gradient, respectively. From Eqs. (6), it follows that, at  $y=\delta$ ,

$$u \rightarrow u^m = u_0^i - \omega_0^i y \quad (7a)$$

$$H \rightarrow H^m = H_0^i + (H_y)_0^i y \quad (7b)$$

In addition, we take  $p \approx p^m$  with

$$p_x^m = -(\rho u^2)_x^m - (\rho uv)_y^m \quad (8)$$

Note the dependence of  $p^m$  on  $y$  implied by Eq. (8) is a higher-order effect.

The effect of the boundary layer on the inviscid flow is obtained by examining the requirements for the matching of the variables in the two regions. From Eq. (1) we obtain

$$\rho v = - \int_0^y (\rho u)_x^m dy + \int_0^y [(\rho u)^m - \rho u]_x dy \quad (9)$$

At  $y=\delta$ ,  $\rho v \rightarrow (\rho v)^m$ ,  $\rho u \rightarrow (\rho u)^m$ , and Eq. (9) gives

$$(\rho v)^m = (\rho v)_0^i - \int_0^y (\rho u)_x^m dy \quad (10)$$

with

$$(\rho v)_0^i = \frac{d}{dx} \int_0^\delta [(\rho u)^m - \rho u] dy \quad (11)$$

Received May 31, 1984; revision received March 20, 1985. This paper is declared a work of the U.S. Government and is not subject to copyright protection in the United States.

\*Acting Chief, Computational Fluid Dynamics Branch.

†Member Technical Staff. Member AIAA.

Equation (11) is the natural generalization of the standard transpiration condition for the case where the effects of a rotational freestream are included in the boundary-layer solution. A similar treatment applied to the streamwise momentum and energy equations (2) and (4) gives

$$(\rho uv)_0^i = \frac{d}{dx} \int_0^\delta [(\rho u^2)^m - \rho u^2] dy - \tau_0 \quad (12)$$

$$(\rho vH)_0^i = \frac{d}{dx} \int_0^\delta [(\rho uH)^m - \rho uH] dy - q_0 \quad (13)$$

Equations (11-13) are the coupling conditions on the normal fluxes of mass, streamwise momentum, and total enthalpy obtained in Ref. 2 by another approach. Note, however, that the quantities  $(\rho u)^m$ ,  $(\rho u^2)^m$ , and  $(\rho uH)^m$  are now functions of  $y$ .

Equations (12) and (13) are now examined further. On introducing Eqs. (7) for  $u^m$  and  $H^m$ , these equations may be rewritten as

$$\begin{aligned} (\rho uv)_0^i &= \frac{d}{dx} \int_0^\delta [(u_0^i - \omega_0^i y) ((\rho u)^m - \rho u) \\ &\quad + \rho u(u^m - u)] dy - \tau_0 = u_0^i \frac{d}{dx} \int_0^\delta [(\rho u)^m - \rho u] dy \\ &\quad + \left\{ (u_x)_0^i \int_0^\delta [(\rho u)^m - \rho u] dy \right. \\ &\quad \left. - \frac{d}{dx} \omega_0^i \int_0^\delta [(\rho u)^m - \rho u] y dy \right. \\ &\quad \left. + \frac{d}{dx} \int_0^\delta \rho u(u^m - u) dy - \tau_0 \right\} \end{aligned} \quad (14)$$

and

$$\begin{aligned} (\rho vH)_0^i &= \frac{d}{dx} \int_0^\delta [(H_0^i + (H_y)_0^i y) ((\rho u)^m - \rho u) \\ &\quad + \rho u(H^m - H)] dy - q_0 = H_0^i \frac{d}{dx} \int_0^\delta [(\rho u)^m - \rho u] dy \\ &\quad + \left\{ (H_x)_0^i \int_0^\delta [(\rho u)^m - \rho u] dy \right. \\ &\quad \left. + \frac{d}{dx} (H_y)_0^i \int_0^\delta [(\rho u)^m - \rho u] y dy \right. \\ &\quad \left. + \frac{d}{dx} \int_0^\delta \rho u(H^m - H) dy - q_0 \right\} \end{aligned} \quad (15)$$

By introducing the integral forms of the momentum and energy equations (see Appendix), it may be shown that the terms in braces in Eqs. (14) and (15) vanish. Hence, if the viscous solution satisfies the boundary-layer equations and the inviscid solution satisfies the normal mass flux condition [Eq. (11)], Eqs. (12) and (13) will also be satisfied independent of the values used for  $u_0^i$  and  $H_0^i$ . Note these same conclusions hold for a first-order boundary-layer solution as can be seen by setting  $\omega_0^i$  and  $(H_y)_0^i$  equal to zero in Eqs. (14) and (15).

Finally, since Eqs. (12) and (13) no longer suffice to determine the inviscid surface values  $u_0^i$  and  $H_0^i$ , we propose a procedure for determining these quantities. First, note that  $u^m$  and  $H^m$ , as given by Eqs. (7), represent both the outer limit of the boundary-layer solution and the inner limit of the inviscid solution. That this is possible is a result of the

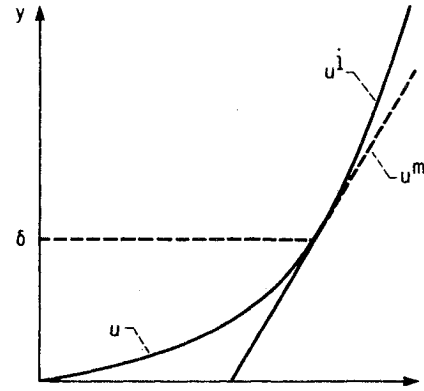


Fig. 1 Matching for thin boundary layer.

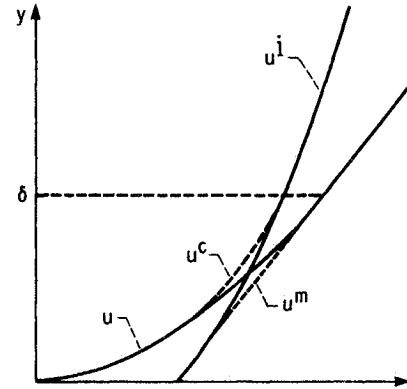


Fig. 2 Matching for thick boundary layer.

existence of an overlap region in which both inner and outer solutions are valid (cf, Ref. 4, Chap. 5). Hence, values of  $u_0^i$  and  $H_0^i$  consistent with these limiting forms can be obtained by linear extrapolation from the inviscid solution adjacent to the wall. When the boundary layer is sufficiently thin so that there is negligible variation in the inviscid vorticity  $\omega^i$  and total enthalpy gradient  $H_y^i$  across the layer, this leads to a smooth blending of the two solutions. This is depicted in Fig. 1. For thick boundary layers, there may be significant variation in  $\omega^i$  and  $H_y^i$  across the layer. In this case, an approximation to the complete solution is obtained from a composite expression

$$u^c = u + u^i - u^m \quad (16)$$

This situation is depicted in Fig. 2. In this latter case, note that the streamline curvature in the outer portion of the boundary layer may produce a significant dependence of  $p^m$  on  $y$  as given by Eq. (8).

### Conclusion

The requirements for coupling a boundary layer and rotational inviscid flow have been re-examined and extended to include the second-order effects of freestream vorticity and total temperature gradient in the boundary-layer analysis. It is shown that if the inviscid solution is computed with the common transpiration condition on the surface normal mass flux used as a boundary condition, then the additional requirements for matching of the normal flux of streamwise momentum and total enthalpy will automatically be satisfied. From the existence of an overlap region of joint validity of both viscous and inviscid solutions, it is then inferred that surface values of inviscid streamwise velocity and total enthalpy can be obtained by linear extrapolation from the inviscid solution adjacent to the wall.

### Appendix

The integral forms of the momentum and energy solutions are obtained below for the case where freestream vorticity and total enthalpy gradients are included in the boundary-layer solution. From Eqs. (1) and (2), and (8),

$$\tau_0 = \int_0^\delta \{u_x^m[(\rho u)^m - \rho u] + [\rho u(u^m - u)]\}_x + u_y^m[(\rho v)^m - \rho v] + [\rho v(u^m - u)]_y dy \quad (A1)$$

Equation (A1) together with Eqs. (1), (10), and (7a) then gives

$$\tau_0 = (u_x)_0^i \int_0^\delta [(\rho u)^m - \rho u] dy - \frac{d}{dx} \omega_0^i \int_0^\delta [(\rho u)^m - \rho u] y dy + \frac{d}{dx} \int_0^\delta \rho u(u^m - u) dy \quad (A2)$$

Similarly, from Eqs. (1), (4), (7b), and (10),

$$q_0 = \int_0^\delta \{H_x^m[(\rho u)^m - \rho u] + [\rho u(H^m - H)]\}_x + H_y^m[(\rho v)^m - \rho v] + [\rho v(H^m - H)]_y dy = (H_x)_0^i \int_0^\delta [(\rho u)^m - \rho u] dy + \frac{d}{dx} (H_y)_0^i \times \int_0^\delta [(\rho u)^m - \rho u] y dy + \frac{d}{dx} \int_0^\delta \rho u(H^m - H) dy \quad (A3)$$

### References

- <sup>1</sup>Melnik, R. E., "Turbulent Interactions on Airfoils at Transonic Speeds—Recent Developments," *Computation of Viscous-Inviscid Interactions*, AGARD CP-291, Oct. 1980, Paper 10.
- <sup>2</sup>Johnston, W. and Sockol, P., "Matching Procedure for Viscous-Inviscid Interactive Calculations," *AIAA Journal*, Vol. 17, June 1979, pp. 661-663.
- <sup>3</sup>Murman, E. M. and Bussing, T.R.A., "On the Coupling of Boundary Layer and Euler Equation Solutions," *2nd Symposium on Numerical and Physical Aspects of Aerodynamic Flows*, 1983, edited by T. Cebeci, Springer-Verlag, New York, 1984, pp. 313-326.
- <sup>4</sup>Van Dyke, M., *Perturbation Methods in Fluid Mechanics*, Academic Press, New York, 1964.

## In-Bore Velocity Measurements in the Wake of a Subsonic Projectile

A.F. Bicen,\* Y. Kliafas,† and J.H. Whitelaw‡  
Imperial College of Science and Technology  
London, England

### Introduction

VELOCITY and pressure have been measured in the flow behind a projectile traveling in a tube and propelled by compressed gas. The arrangement is intended to simulate that

Received April 10, 1985; presented as Paper 85-1676 at the AIAA 18th Fluid Dynamics, Plasmadynamics and Lasers Conference, Cincinnati, OH, July 16-18, 1985; revision received Aug. 26, 1985. Copyright © American Institute of Aeronautics and Astronautics, Inc., 1985. All rights reserved.

\*Research Fellow, Department of Mechanical Engineering.

†Research Assistant, Department of Mechanical Engineering. Member AIAA.

‡Professor, Department of Mechanical Engineering.

of interior ballistics, with nonreacting flow and projectile velocities up to 21 m/s. Although the real processes are much more complex and involve a continuous interaction of two phases (solid gas or liquid gas) through a combustion process, the present simplified experiments serve to provide fundamental understanding of the flow behind in-bore projectiles and thereby support the development of phenomenological models, such as those of Refs. 1 and 2, and multidimensional solution methods such as that of Ref. 3.

A projectile was secured in position inside a tube pressurized by compressed gas to a required pressure. After the gas had become quiescent, the projectile was released. The pressure in the tube and the projectile velocity were measured, together with the local velocity of the fluid obtained with a laser velocimeter, as a function of time. The experiment was repeated at different locations until a satisfactory picture of the flow had been assembled. The initial pressure was regarded as a variable so as to determine the extent to which the flow properties varied with projectile velocity, and the experiment was conducted with two initial chambers of different length.

### Experimental System

The flow arrangement and related instrumentation are shown in Fig. 1. The measurements were obtained in the cavity formed by a 76.7-mm-diam tube, a blanked end, and a 76.4-mm-diam projectile that had a flat end. The effect of initial chamber length was investigated by using two different lengths of 177.3 and 311 mm, which were achieved by altering the projectile overall length. The upper 300 mm of the tube was made of plexiglass and the remaining part of mild steel with the gap between the projectile and tube wall sealed by two silicon-rubber rings. The projectile was allowed to travel for a distance of approximately 400 mm before being retarded by a series of compression springs.

The initial gas pressure  $P_i$  ranged from 2.91 to 9.1 bars and was achieved with nitrogen taken from a pressurized cylinder.

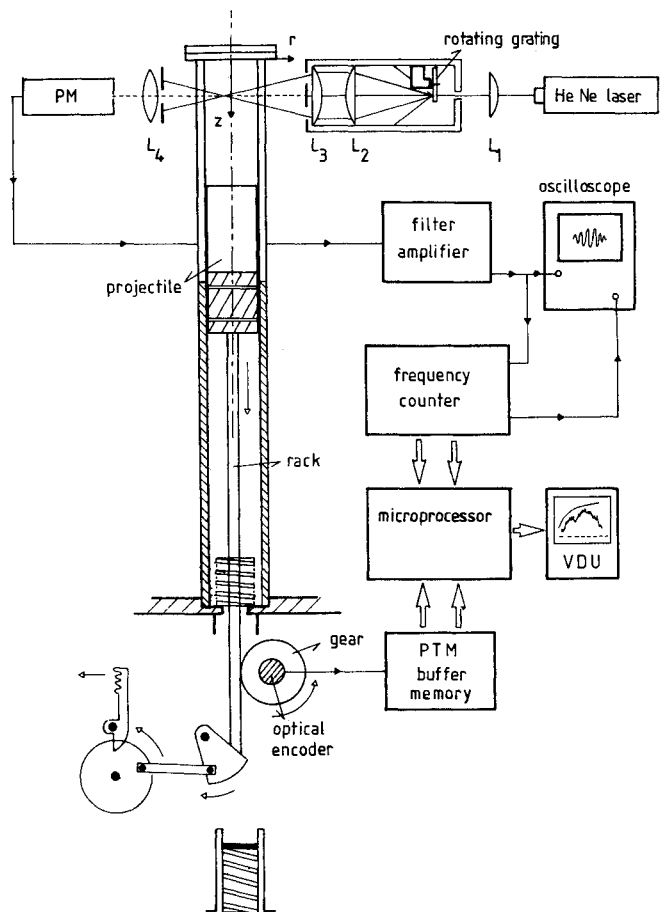


Fig. 1 Schematic diagram of experimental system.